INSTITUTE OF PHYSICS PUBLISHING JOURNAL OF PHYSICS: CONDENSED MATTER

J. Phys.: Condens. Matter **13** (2001) 3643–3654 www.iop.org/Journals/cm PII: S0953-8984(01)19606-2

Charge current in ferromagnet–triplet-superconductor junctions

N Stefanakis

Department of Physics, University of Crete, PO Box 2208, GR-71003, Heraklion, Crete, Greece

Received 28 November 2000, in final form 6 February 2001

Abstract

We calculate the tunnelling conductance spectra of a ferromagnetic metal/insulator/triplet-superconductor junction from the reflection amplitudes using the Blonder–Tinkham–Klapwijk formula. For the triplet superconductor, we assume one special p-wave order parameter, having line nodes, and two two-dimensional f-wave order parameters with line nodes, breaking the time-reversal symmetry. Also we examine nodeless pairing potentials. The evolution of the spectra with the exchange potential depends solely on the topology of the gap. The weak Andreev reflection within the ferromagnet results in the suppression of the tunnelling conductance and eliminates the resonances due to the anisotropy of the pairing potential. The tunnelling spectrum splits asymmetrically with respect to $E = 0$ under the influence of an external magnetic field. The results can be used to distinguish between the possible candidate pairing states of the superconductor Sr_2RuO_4.

1. Introduction

The recent discovery of superconductivity in Sr_2RuO_4 has attracted much theoretical and experimental interest [1]. The time-reversal symmetry is broken for the superconductor Sr_2RuO_4, and the magnetic field is spontaneously induced as shown by μSR experiment [2]. The Knight shift shows no change when passing through the superconducting state and this is a clear indication of a spin-triplet pairing state, with a $\boldsymbol{d}$-vector aligned with the z-axis [3]. In addition, the band-structure calculations [4] and de Haas–van Alphen measurements [5] show little dispersion along k_z, which is consistent with a two-dimensional basis function on a cylindrical Fermi surface. Furthermore, the presence of a large residual density of states of quasiparticles inside the superconducting gap is evident from the linear temperature dependence of the nuclear spin–lattice relaxation rate $1/T_1$ of ^{101}Ru below 0.4 K [6]. Also, specific heat measurements support the scenario of line nodes within the gap, as in the high-T_c cuprate superconductors [7].

In the experiments on tunnelling between normal metals and superconductors, Andreev reflection processes take place [8,9]. In the Andreev reflection process an electron incident on the barrier with an energy below the gap cannot drain off into the superconductor. It is instead reflected as a hole and a Cooper pair is transferred into the superconductor. In anisotropic

0953-8984/01/153643+12$30.00

high-T_c superconductors, due to the sign change of the pair potential that the transmitted quasiparticles experience, zero-energy states are formed, which are detected as peaks in the conductance spectra at $E = 0$ [10]. Also, in the presence of an imaginary s-wave component, which breaks the time-reversal symmetry, the zero-energy peak is shifted to the amplitude of the subdominant component [11, 12].

The properties of the Andreev reflection are modified in the presence of an exchange field such as in ferromagnet/insulator/superconductor junctions, since the back-reflection of the Andreev reflection is suppressed in the ferromagnet. This phenomenon has been clarified both in s-wave and in d-wave junctions and interesting aspects of the Andreev reflection have been revealed [13–16]. Also the properties of ferromagnet/insulator/triplet-superconductor junctions have been studied where two types of pairing potential are assumed for the triplet superconductor, i.e. the unitary and the non-unitary types with E_u symmetry [17]. In the unitary case the conductance within the gap is reduced by the exchange interaction while in the non-unitary case it is not much influenced since the latter pairing state conserves spin.

In order to identify the pairing state of Sr_2RuO_4 the Bogoliubov–de Gennes (BdG) equations have been used to calculate the quasiparticle bound-state wave function around non-magnetic impurities in unconventional superconductors [18]. The characteristic patterns were distinguished for two proposed symmetries of the order parameters, namely: (i) E_u; and (ii) $B_{1g} \times E_u$.

In this paper we will use the BdG equations to calculate the tunnelling conductance of ferromagnet/triplet-superconductor contacts, with a barrier of arbitrary strength between them, in terms of the probability amplitudes of Andreev and normal reflection. For the triplet superconductor we shall assume three possible pairing states of two-dimensional order parameters, having line nodes within the RuO_2 plane, which break the time-reversal symmetry. The first two are the 2D f-wave states proposed by Hasegawa *et al* [19] having $B_{1g} \times E_u$ and $B_{2g} \times E_u$ symmetry. The other one is called the nodal p-wave state and has been proposed by Dahm *et al* [20]; here the pairing potential has the form $\boldsymbol{d}(\boldsymbol{k}) = \Delta_0 \hat{\boldsymbol{z}}(\sin(k_x a) + \mathrm{i}\sin(k_y a))$, with $k_x a = \pi\cos\theta$, $k_y a = \pi\sin\theta$. This pairing symmetry has nodes as in the $B_{2g} \times E_u$ case. Also we will consider two nodeless pairing states. One is the isotropic p-wave state and the other is the nodeless p-wave state initially proposed by Miyake and Narikiyo [21], both breaking the time-reversal symmetry. Generally the tunnelling conductance is suppressed with the increase of the exchange interaction and the peaks are removed. This is due to the suppression of the Andreev reflection in the ferromagnet. For the nodal pairing states the linear dependence of the tunnelling conductance on E is not much influenced. For the nodeless cases, the normalized conductance develops a constant value within the gap, which becomes suppressed as the exchange field gets larger. When the ferromagnet is a normal metal, the magnetic field splits the tunnelling spectrum symmetrically around $E = 0$. The exchange field eliminates the negative branch of the tunnelling spectra in the half-metallic ferromagnetic limit.

2. Theory of the tunnelling effect

For spin-triplet superconductors the wave functions describing the quasiparticles $\hat{\Psi}(\boldsymbol{r})$ are four-spinors in Nambu (particle–hole $\otimes$ spin) space. Their particle and hole components are determined by the solutions of the BdG equations [23, 24]:

$$E\hat{\Psi}(\boldsymbol{r}) = \int \mathrm{d}\boldsymbol{r}'\ \hat{H}(\boldsymbol{r}, \boldsymbol{r}')\hat{\Psi}(\boldsymbol{r}') \tag{1}$$

where

$$\hat{\Psi}(\boldsymbol{r}) = \begin{pmatrix} u_\uparrow(\boldsymbol{r}) \\ u_\downarrow(\boldsymbol{r}) \\ v_\uparrow(\boldsymbol{r}) \\ v_\downarrow(\boldsymbol{r}) \end{pmatrix} \tag{2}$$

$$\hat{H}(\boldsymbol{r}, \boldsymbol{r}') = \begin{pmatrix} \hat{H}_e & \hat{\Delta} \\ \hat{\Delta}^* & -\hat{H}_e \end{pmatrix}. \tag{3}$$

$\hat{\Delta}$ is the 2×2 triplet pairing matrix with elements of the form $\Delta_{s\bar{s}}(\boldsymbol{r}, \boldsymbol{r}')$, and the spin index $s = \uparrow$ or $s = \downarrow$. $\hat{H}_e = H_e(\boldsymbol{r}')\delta(\boldsymbol{r} - \boldsymbol{r}')\hat{o}_0$, where $\hat{o}_0$ is the 2×2 unit matrix, and $\mathcal{H}_e(\boldsymbol{r})$ is the single-particle Hamiltonian which is given by $\mathcal{H}_e(\boldsymbol{r}) = -\hbar^2\nabla_{\boldsymbol{r}}^2/2m_e + V(\boldsymbol{r}) - E_F$; E is the energy measured from the Fermi energy E_F. For the pairing states that we examine in section 3, the spin-up and spin-down components decouple. We will consider only triplet pairing states where $\Delta_{\uparrow\uparrow}(\boldsymbol{r}, \boldsymbol{r}') = \Delta_{\downarrow\downarrow}(\boldsymbol{r}, \boldsymbol{r}') = 0$, while $\Delta_{\uparrow\downarrow}(\boldsymbol{r}, \boldsymbol{r}') = \Delta_{\downarrow\uparrow}(\boldsymbol{r}, \boldsymbol{r}')$. In that case the Cooper pairs have zero spin projection. The spin-dependent BdG equations are decoupled into two independent sets of (two-component) equations, one for the spin-up-electron, spin-down-hole quasiparticle $(u_\uparrow(\boldsymbol{r}), v_\downarrow(\boldsymbol{r}))$, and the other for $(u_\downarrow(\boldsymbol{r}), v_\uparrow(\boldsymbol{r}))$. The corresponding BdG equations for spin index s $(\bar{s}) = \uparrow (\downarrow)$ or s $(\bar{s}) = \downarrow (\uparrow)$ read [25]

$$\begin{aligned} E u_s(\boldsymbol{r}) &= (\mathcal{H}_e(\boldsymbol{r}) - \rho U(\boldsymbol{r}))u_s(\boldsymbol{r}) + \int \mathrm{d}\boldsymbol{r}'\ \Delta_{s\bar{s}}(\boldsymbol{s}, \boldsymbol{x})v_{\bar{s}}(\boldsymbol{r}') \\ E v_{\bar{s}}(\boldsymbol{r}) &= -(\mathcal{H}_e^*(\boldsymbol{r}) + \rho U(\boldsymbol{r}))v_{\bar{s}}(\boldsymbol{r}) + \int \mathrm{d}\boldsymbol{r}'\ \Delta_{\bar{s}s}^*(\boldsymbol{s}, \boldsymbol{x})u_s(\boldsymbol{r}') \end{aligned} \tag{4}$$

where $U(\boldsymbol{r})$ is the exchange potential, ρ is 1 (-1) for up (down) spins. $\Delta_{s\bar{s}}(\boldsymbol{s}, \boldsymbol{x})$ is the matrix element of the pair potential, after a transformation from the position coordinates $\boldsymbol{r}, \boldsymbol{r}'$ to the centre-of-mass coordinate $\boldsymbol{x} = (\boldsymbol{r} + \boldsymbol{r}')/2$, and the relative vector $\boldsymbol{s} = \boldsymbol{r} - \boldsymbol{r}'$. After Fourier transformation the pair potential depends on the related wave vector $\boldsymbol{k}$ and $\boldsymbol{x}$. In the weak-coupling limit, $\boldsymbol{k}$ is fixed to being on the Fermi surface $(|\boldsymbol{k}| = k_F)$, and only its direction θ is variable. After applying the quasi-classical approximation, i.e.

$$\begin{pmatrix} \bar{u}_s(\boldsymbol{r}) \\ \bar{v}_{\bar{s}}(\boldsymbol{r}) \end{pmatrix} = \mathrm{e}^{-\mathrm{i}\boldsymbol{k}\cdot\boldsymbol{r}} \begin{pmatrix} u_s(\boldsymbol{r}) \\ v_{\bar{s}}(\boldsymbol{r}) \end{pmatrix} \tag{5}$$

so that the fast-oscillating part of the wave function is divided out, the BdG equations are reduced to the Andreev equations [9]:

$$\begin{aligned} E\bar{u}_s(\boldsymbol{r}) &= -(\mathrm{i}\hbar^2/m)\boldsymbol{k}\cdot\boldsymbol{\nabla}\bar{u}_s(\boldsymbol{r}) + \Delta_{s\bar{s}}(\theta, \boldsymbol{r})\bar{v}_{\bar{s}}(\boldsymbol{r}) \\ E\bar{v}_{\bar{s}}(\boldsymbol{r}) &= (\mathrm{i}\hbar^2/m)\boldsymbol{k}\cdot\boldsymbol{\nabla}\bar{v}_{\bar{s}}(\boldsymbol{r}) + \Delta_{\bar{s}s}^*(\theta, \boldsymbol{r})\bar{u}_s(\boldsymbol{r}) \end{aligned} \tag{6}$$

where the quantities $\bar{u}_s(\boldsymbol{r})$ and $\bar{v}_{\bar{s}}(\boldsymbol{r})$ are electronlike and holelike quasiparticles with spin indices s and $\bar{s}$ respectively.

We consider the ferromagnet/insulator/superconductor junction shown in figure 1. The geometry of the problem has the following limitations. The particles move in the xy-plane and the boundary between the ferromagnet $(x < 0)$ and superconductor $(x > 0)$ is the yz-plane at $x = 0$. The insulator is modelled by a delta function, located at $x = 0$, of the form $V\delta(x)$. The temperature is fixed at 0 K. We take both the pair potential and the exchange energy as step functions, i.e. $\Delta_{s\bar{s}}(\theta, \boldsymbol{r}) = \Theta(x)\Delta_{s\bar{s}}(\theta)$, $U\boldsymbol{r}) = \Theta(-x)U$. For the geometry shown in figure 1, equations (6) take the form

$$\begin{aligned} E\bar{u}_s(x) &= -(\mathrm{i}\hbar^2/m)k_{Fx}\frac{\mathrm{d}}{\mathrm{d}x}\bar{u}_s(x) + \Delta_{s\bar{s}}(\theta)\bar{v}_{\bar{s}}(x) \\ E\bar{v}_{\bar{s}}(x) &= (\mathrm{i}\hbar^2/m)k_{Fx}\frac{\mathrm{d}}{\mathrm{d}x}\bar{v}_{\bar{s}}(x) + \Delta_{\bar{s}s}^*(\theta)\bar{u}_s(x). \end{aligned} \tag{7}$$

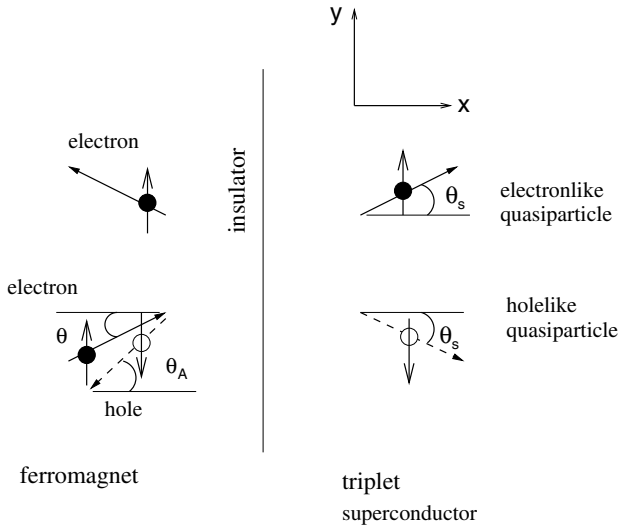

Figure 1. The geometry of the ferromagnet/insulator/triplet-superconductor interface. The pairing state is unitary with zero spin projection. The vertical line along the y-axis represents the insulator. The arrows illustrate the transmission and reflection processes at the interface. θ is the angle of the incident electron and the normal, θ_A is the angle of the reflected hole and the normal, and θ_s is the angle of the transmitted quasiparticle and the normal. Note that θ is not equal to θ_A since the back-reflection of the Andreev process is suppressed.

When a beam of electrons is incident from the ferromagnet to the insulator, at an angle θ, the general solution of equations (7) is the two-component wave function $\Psi_{\rm I} = (u_{\uparrow[\downarrow]}, v_{\downarrow[\uparrow]})$ which for $x < 0$ is written as

$$\Psi_{\rm I} = \begin{pmatrix} 1 \\ 0 \end{pmatrix} {\rm e}^{{\rm i}q_{\uparrow[\downarrow]}x\cos\theta} + a_{\uparrow[\downarrow]} \begin{pmatrix} 0 \\ 1 \end{pmatrix} {\rm e}^{{\rm i}q_{\downarrow[\uparrow]}x\cos\theta_A} + b_{\uparrow[\downarrow]} \begin{pmatrix} 1 \\ 0 \end{pmatrix} {\rm e}^{-{\rm i}q_{\uparrow[\downarrow]}x\cos\theta} \tag{8}$$

where $a_{\uparrow[\downarrow]}, b_{\uparrow[\downarrow]}$ are the amplitudes for Andreev and normal reflections for spin-up (spin-down) quasiparticles, and

$$q_{\uparrow[\downarrow]} = \sqrt{\frac{2m}{\hbar^2}(E_F \pm U)}$$

is the wave vector of quasiparticles in the ferromagnet for up (down) spin. The wave vector of the electronlike and holelike quasiparticles is approximated by $k_s = \sqrt{(2mE_F/\hbar^2)}$. Since the translational symmetry holds in the y-axis direction, the momentum parallel to the interface is conserved, i.e. $q_\uparrow \sin\theta = q_\downarrow \sin\theta_A = k_s \sin\theta_s$. Note that θ is different to θ_A since the back-reflection of the Andreev reflection is suppressed. Using the matching conditions of the wave function at $x = 0$, $\Psi_{\rm I}(0) = \Psi_{\rm II}(0)$ and $\Psi'_{\rm II}(0) - \Psi'_{\rm I}(0) = (2mV/\hbar^2)\Psi_{\rm I}(0)$, the Andreev and normal reflection amplitudes $a_{\uparrow[\downarrow]}, b_{\uparrow[\downarrow]}$ for the spin-up (spin-down) quasiparticles are obtained ($\mathcal{A}$ is standing for $n_+n_-\phi_-\phi_+^*$):

$$a_{\uparrow[\downarrow]} = \frac{4n_+\lambda_1}{(-1-\lambda_1-{\rm i}z_{\uparrow[\downarrow]})(-1-\lambda_2+{\rm i}z_{\uparrow[\downarrow]}) + (1-\lambda_1-{\rm i}z_{\uparrow[\downarrow]})(-1+\lambda_2-{\rm i}z_{\uparrow[\downarrow]})\mathcal{A}} \tag{9}$$

$$b_{\uparrow[\downarrow]} = \frac{(-1-\lambda_2+{\rm i}z_{\uparrow[\downarrow]})(1-\lambda_1+{\rm i}z_{\uparrow[\downarrow]}) + (-1+\lambda_2-{\rm i}z_{\uparrow[\downarrow]})(-1-\lambda_1+{\rm i}z_{\uparrow[\downarrow]})\mathcal{A}}{(-1-\lambda_1-{\rm i}z_{\uparrow[\downarrow]})(-1-\lambda_2+{\rm i}z_{\uparrow[\downarrow]}) + (1-\lambda_1-{\rm i}z_{\uparrow[\downarrow]})(-1+\lambda_2-{\rm i}z_{\uparrow[\downarrow]})\mathcal{A}} \tag{10}$$

where

$$z_0 = \frac{mV}{\hbar^2 k_s} \qquad z_{\uparrow[\downarrow]} = \frac{2z_0}{\cos\theta_s} \qquad \lambda_1 = \frac{\cos\theta}{\cos\theta_s}\frac{q_{\uparrow[\downarrow]}}{k_s} \qquad \lambda_2 = \frac{\cos\theta_A}{\cos\theta_s}\frac{q_{\downarrow[\uparrow]}}{k_s}.$$

The BCS coherence factors are given by

$$u_{\pm}^2 = [1 + \sqrt{E^2 - |\Delta_{\pm}(\theta)|^2}/E]/2 \tag{11}$$

$$v_{\pm}^2 = [1 - \sqrt{E^2 - |\Delta_{\pm}(\theta)|^2}/E]/2 \tag{12}$$

and $n_{\pm} = v_{\pm}/u_{\pm}$. The internal phase arising from the energy gap is given by $\phi_{\pm} = [\Delta_{\pm}(\theta)/|\Delta_{\pm}(\theta)|]$, where $\Delta_{+}(\theta) = \Delta(\theta)$ ($\Delta_{-}(\theta) = \Delta(\pi - \theta)$) is the pair potential experienced by the transmitted electronlike (holelike) quasiparticle. $\Delta(\theta) = \Delta_{\uparrow\downarrow}(\theta) = \Delta_{\downarrow\uparrow}(\theta)$, since the Cooper pairs have zero spin projection, i.e. $\boldsymbol{d} \parallel \hat{\boldsymbol{z}}$.

When $\theta > \sin^{-1}(k_s/q_{\uparrow}) \equiv \theta_{c1}$ total reflection occurs and the spin and charge current vanishes. When $\theta_{c1} > \theta > \sin^{-1}(q_{\uparrow}/q_{\downarrow}) \equiv \theta_{c2}$, although the transmitted quasiparticles in the superconductor do propagate, the Andreev-reflected quasiparticles do not propagate. This process is called virtual Andreev reflection (VAR). In this case the spin and charge current do not vanish since a finite amplitude of the Andreev reflection still exists [15].

According to the Blonder–Tinkham–Klapwijk (BTK) formula the conductance for the charge current of the junction, $\bar{\sigma}_{q_{\uparrow[\downarrow]}}(E, \theta)$, for up-spin (down-spin) quasiparticles, is expressed in terms of the probability amplitudes $a_{\uparrow[\downarrow]}$, $b_{\uparrow[\downarrow]}$ as [8, 15]

$$\bar{\sigma}_{q_{\uparrow[\downarrow]}}(E, \theta) = \mathrm{Re}\left[1 + \frac{\lambda_2}{\lambda_1}|a_{\uparrow[\downarrow]}|^2 - |b_{\uparrow[\downarrow]}|^2\right]. \tag{13}$$

The tunnelling conductance, normalized by that in the normal state, is given by

$$\sigma_q(E) = \sigma_{q_{\uparrow}}(E) + \sigma_{q_{\downarrow}}(E) \tag{14}$$

$$\sigma_{q_{\uparrow[\downarrow]}}(E) = \frac{1}{R_N}\int_{-\pi/2}^{\pi/2} \mathrm{d}\theta\, \cos\theta\, \bar{\sigma}_{q_{\uparrow[\downarrow]}}(E, \theta) P_{\uparrow[\downarrow]} q_{\uparrow[\downarrow]} \tag{15}$$

where

$$R_N = \int_{-\pi/2}^{\pi/2} \mathrm{d}\theta\, \cos\theta [\sigma_{N_{\uparrow}}(\theta) P_{\uparrow} q_{\uparrow} + \sigma_{N_{\downarrow}}(\theta) P_{\downarrow} q_{\downarrow}] \tag{16}$$

$$\sigma_{N_{\uparrow[\downarrow]}}(\theta) = \frac{4\lambda_1}{(1+\lambda_1)^2 + z_{\uparrow[\downarrow]}^2} \tag{17}$$

where $P_{\uparrow[\downarrow]} = (E_F \pm U)/2E_F$ is the polarization for up (down) spin. In the $z_0 = 0$ limit the interface is regarded as a weak link, showing metallic behaviour, while for large z_0-values, the interface becomes insulating.

3. Possible spin-triplet pairing states

For the spin-triplet pairing state the Cooper pairs have one spin degree of freedom. The gap function is a 2×2 symmetric matrix which in the spin space can be written as

$$\hat{\Delta}(\boldsymbol{k}) = \mathrm{i}\sigma_y(\boldsymbol{d}(\boldsymbol{k}) \cdot \hat{\boldsymbol{\sigma}}) \tag{18}$$

where $\hat{\boldsymbol{\sigma}}$ denotes the Pauli matrices and $\boldsymbol{d}(\boldsymbol{k})$ is a vectorial function which is odd in $\boldsymbol{k}$. The $\boldsymbol{d}$-vector defines the axis along which the Cooper pairs have zero spin projection. In the following we will take $\boldsymbol{d} \parallel \hat{\boldsymbol{z}}$. In that case $\Delta_{\uparrow\uparrow} = \Delta_{\downarrow\downarrow} = 0$, while $\Delta_{\uparrow\downarrow} = \Delta_{\downarrow\uparrow} = \Delta(\theta)$. The energy spectrum of the quasiparticles consists of two branches which are identical for unitary pairing states—i.e. $\hat{\Delta}^{\dagger}(\boldsymbol{k})\hat{\Delta}(\boldsymbol{k})$ is proportional to the unit matrix—and distinct for non-unitary states. The non-unitary states have been ruled out for Sr_2RuO_4 by the very small residual value of the specific heat at zero temperature [7]. In this paper we will examine only the case of unitary pairing states. As an example we consider the state

$$\hat{\Delta}(\theta) = \Delta_0 \begin{pmatrix} \Delta_{\uparrow\uparrow}(\theta) & \Delta_{\uparrow\downarrow}(\theta) \\ \Delta_{\downarrow\uparrow}(\theta) & \Delta_{\downarrow\downarrow}(\theta) \end{pmatrix}. \tag{19}$$

(a) For the isotropic p-wave pairing state, $\Delta_{\uparrow\downarrow}(\theta) = \Delta_{\downarrow\uparrow}(\theta) = \Delta_0 \exp(\mathrm{i}(\theta - \beta))$ and $\Delta_{\uparrow\uparrow}(\theta) = \Delta_{\downarrow\downarrow}(\theta) = 0$; β denotes the angle between the normal to the interface and the x-axis of the crystal. This is an opposite-spin pairing state, with a gap of constant modulus for both spin parts on the Fermi surface. In the following we will consider the cases where the matrix element $\Delta_{\uparrow\downarrow}(\theta)$ (expressed as $\Delta(\theta)$) of equation (19) has the following θ-dependences.

(b) In the case of a p-wave superconductor, proposed by Miyake and Narikiyo [21]

$$\Delta(\theta) = \frac{\Delta_0}{s_M}[\sin(k_x a) + \mathrm{i}\sin(k_y a)] \tag{20}$$

with $k_x a = R\pi\cos(\theta - \beta)$ and $k_y a = R\pi\sin(\theta - \beta)$, $s_M = \sqrt{2}\sin(\pi/\sqrt{2}) = 1.125$, and $R = 0.9$. This state does not have nodes.

We consider also three pairing symmetries for Sr_2RuO_4 with line nodes.

(c) In the first 2D f-wave state $B_{1g} \times E_u$,

$$\Delta(\theta) = \Delta_0 \cos 2(\theta - \beta)[\cos(\theta - \beta) + \mathrm{i}\sin(\theta - \beta)]. \tag{21}$$

This state has nodes at the same points as in the $d_{x^2-y^2}$-wave case.

(d) For the second 2D f-wave state $B_{2g} \times E_u$,

$$\Delta(\theta) = \Delta_0 \sin 2(\theta - \beta)[\cos(\theta - \beta) + \mathrm{i}\sin(\theta - \beta)]. \tag{22}$$

This state has nodes at $0, \pi/2, \pi, 3\pi/2$, and has also been studied by Graf and Balatsky [22].

(e) In case of a nodal p-wave superconductor,

$$\Delta(\theta) = \frac{\Delta_0}{s_M}[\sin(k_x a) + \mathrm{i}\sin(k_y a)] \tag{23}$$

with $k_x a = \pi\cos(\theta - \beta)$ and $k_y a = \pi\sin(\theta - \beta)$. We use here the same normalization as was proposed by Dahm *et al* [20]: $s_M = \sqrt{2}\sin(\pi/\sqrt{2}) = 1.125$, where the Fermi wave vector is chosen as $k_F a = \pi$, in order to have a node in $\Delta(\theta)$. This state has nodes as in the $B_{2g} \times E_u$ state. The corresponding nodeless form was initially proposed by Miyake and Narikiyo [21] and is considered as a separate case.

4. Tunnelling conductance characteristics

In figures 2–6 we plot the tunnelling conductance $\sigma_q(E)$ for different values of the exchange interaction $x = U/E_F$: (a) $z_0 = 0$, $\beta = 0$, (b) $z_0 = 2.5$, $\beta = 0$, (c) $z_0 = 2.5$, $\beta = \pi/4$. The pairing symmetry of the superconductor is $B_{1g} \times E_u$ in figure 2, $B_{2g} \times E_u$ in figure 3, nodal p wave in figure 4, the p wave proposed by Miyake and Narikiyo [21] in figure 5, and isotropic p wave in figure 6. When the ferromagnet is a normal metal, i.e. $x = 0$, the results of [26] are reproduced. For $z_0 = 0$, the subgap conductance becomes suppressed with the increase of x, as in the case of a $d_{x^2-y^2}$-wave superconductor [15].

In the case of a normal-metal/insulator/triplet-superconductor junction the peaks inside the gap are connected to bound states, which are formed due to the sign change that the transmitted quasiparticles feel, for fixed β at discrete values of θ. The conductance peaks occur at these energies where an increased number of bound states are formed [26]. For unitary pairing states the spins of the incident electron and the Andreev-reflected hole are opposite and, since the spin-up and spin-down quasiparticles have equal wave vectors, no spin effects are involved in the Andreev reflection. This is not true when the normal metal is replaced by a ferromagnet. In that case the spin-up and spin-down wave vectors are not equal and the

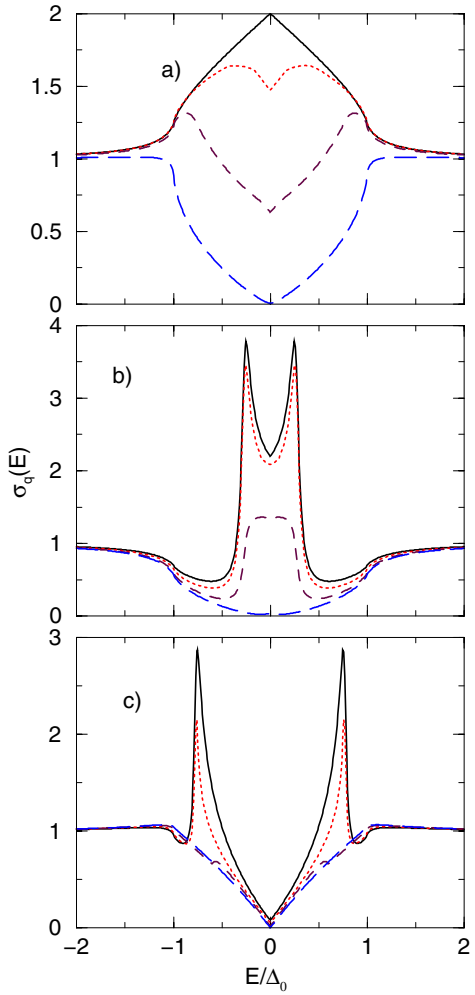

Figure 2. The normalized tunnelling conductance $\sigma_q(E)$ as a function of E/Δ_0 for $x = 0$ (solid line), $x = 0.4$ (dotted line), $x = 0.8$ (dashed line), and $x = 0.999$ (long-dashed line), for different orientations: (a) $Z = 0$, $\beta = 0$, (b) $Z = 2.5$, $\beta = 0$, (c) $Z = 2.5$, $\beta = \pi/4$. The pairing symmetry of the superconductor is $B_{1g} \times E_u$.

spin affects the Andreev reflection. The Andreev-reflected hole decays in the ferromagnet and the interference with the reflected electron is weak. Moreover the transmitted quasiparticles experience weakly the sign change of the pair potential, which is the reason for the formation of the conductance peak. Due to this the conductance peaks are suppressed. This is seen in figures 2(b) and 2(c), with $z_0 = 2.5$ and $\beta = 0$ $(\pi/4)$, for the $B_{1g} \times E_u$ case. Quantitatively the suppression of the conductance peaks in the ferromagnet/insulator/triplet-superconductor junction can be seen if we calculate the magnitude of the Andreev-reflected amplitude as a function of the exchange field when a bound state is formed. Then the amplitude would decay to zero with the increase of the exchange field. This calculation has been done in the case of a ferromagnet/insulator/time-reversal-symmetry-broken-superconductor junction where simple arguments have been derived to connect the suppression of the Andreev reflection as x increases with the reduction of the conductance peaks [27].

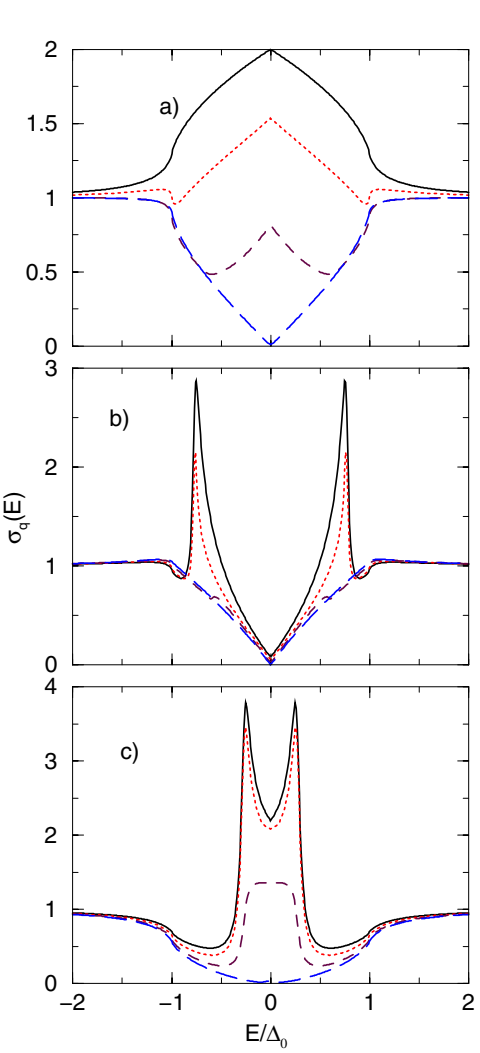

Figure 3. The same as figure 2, but the pairing symmetry of the superconductor is $B_{2g} \times E_u$.

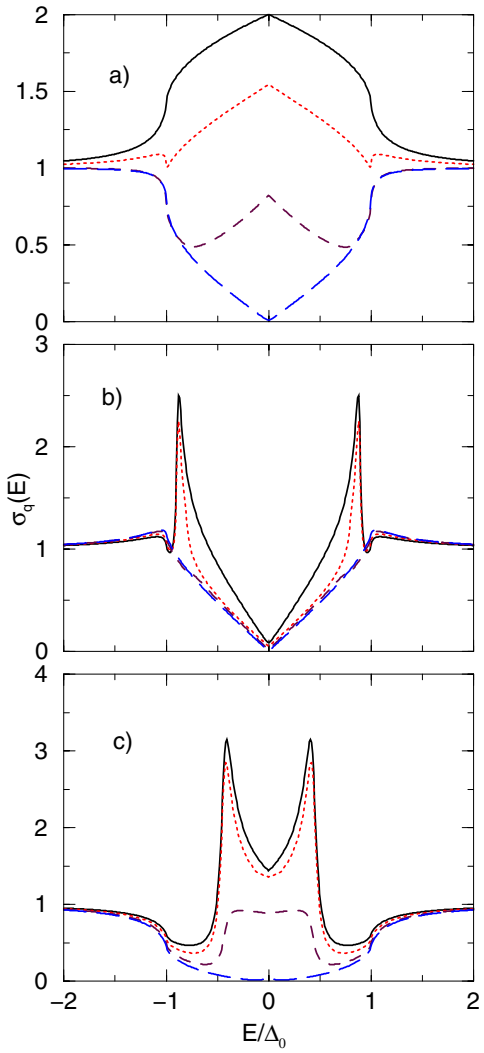

Figure 4. The same as figure 2, but the pairing symmetry of the superconductor is nodal p wave.

Also in the metallic limit ($x = 0$), for all pairing states we see the presence of a large residual density of states within the energy gap as a signature of unconventional pairing symmetry with higher-than-two angular momentum. This is modified by the presence of the ferromagnet, where the increase of the exchange field suppresses the density of states within the gap. Also in the metallic limit the conductance increases linearly with E, which is consistent with the presence of line nodes in the pairing potential. This linear form of the spectra remains unchanged when increasing x. Generally the evolution of the conductance spectra with the increase of x, for the three pairing symmetries with line nodes, depends strongly on the position of the nodes in the pairing potential. In the $d_{x^2-y^2}$-wave case the peak at $E = 0$ and $\beta = \pi/4$, due to the sign change of the pairing potential for the transmitted quasiparticles, is substantially reduced with the increase of x [15]. In the case of the $(B_{1g} \times E_u)$-wave state for $x = 0$, the pairing potential is more complicated and the sign change occurs at discrete values

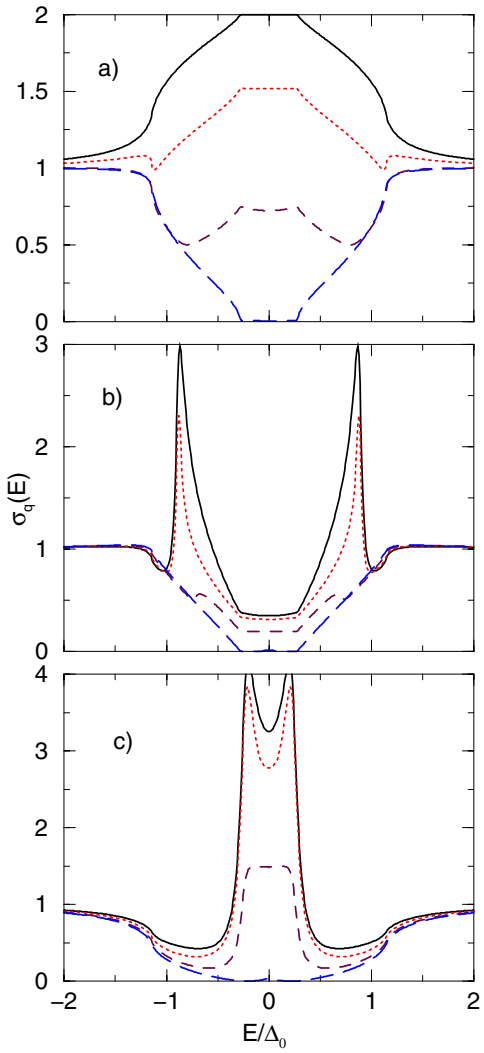

Figure 5. The same as figure 2, but the pairing symmetry of the superconductor is the p wave proposed by MN.

of θ, for fixed β. As a result bound states are formed within the gap, and also the position of the conductance peaks depends on the orientation angle β, as seen in figure 2. Also the spectrum for angle β in the $B_{1g} \times E_u$ case is identical to the spectrum for $B_{2g} \times E_u$ in figure 3 for the angle $\pi/4 - \beta$, since the nodes for the two symmetries differ by $\pi/4$. The evolution with x of the conductance spectra for $z_0 = 0$ is different in the $B_{1g} \times E_u$ and $B_{2g} \times E_u$ cases. It develops a dip at $E = 0$ in the $B_{1g} \times E_u$ case, while it has a peak in the $B_{2g} \times E_u$ case, at $E = 0$. The nodal p-wave case in figure 4 has the same nodal structure as the $B_{2g} \times E_u$ case and we see that the spectra for these two candidates are similar.

For nodeless pairing states a subgap or a full gap opens in the tunnelling spectra. This is seen in figure 5, for the pairing state proposed by Miyake and Narikiyo (MN) [21]. The spectrum is similar to that for the nodal p-wave case, except that in the MN case a subgap opens in the tunnelling spectra for a certain junction orientation. In this region, for $z_0 = 0$

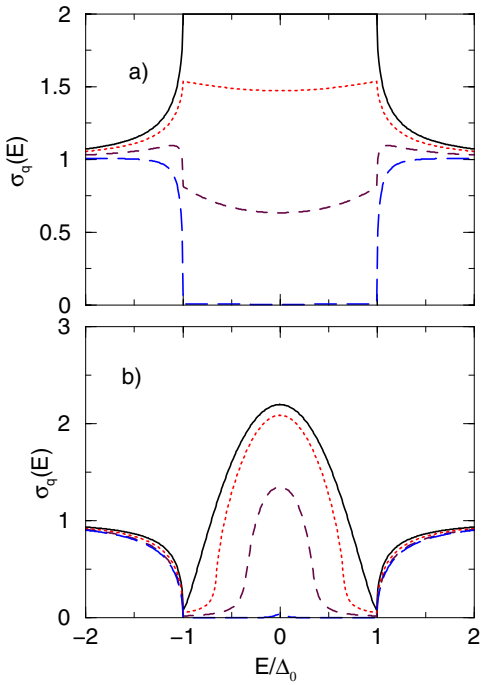

Figure 6. Normalized tunnelling conductance $\sigma_q(E)$ as a function of E/Δ_0 for $x = 0$ (solid line), $x = 0.4$ (dotted line), $x = 0.8$ (dashed line), and $x = 0.999$ (long-dashed line), for different orientations: (a) $z_0 = 0$, $\beta = 0$, (b) $z_0 = 2.5$, $\beta = 0$. The pairing symmetry of the superconductor is isotropic p wave.

the tunnelling conductance is equal to 2 when $x = 0$, and has a constant value for $x > 0$. The tiny subgap is an indication of the nodeless pairing state. For the isotropic p-wave case the tunnelling spectrum changes with z_0, as can be seen in figure 6, but not with the boundary orientation β. The spectrum is nodeless, and for $z_0 = 0$, the conductance is $\sigma_q(E) = 2$, within the energy gap, for $x = 0$. Similar results have been obtained in reference [17], where the tunnelling conductance of a ferromagnet/triplet-superconductor interface is calculated, for both unitary and non-unitary pairing states, having E_u symmetry. Generally in all pairing states the reduction of the subgap conductance with the exchange field is symmetric since the density-of-states modulation within the subgap is not induced by spin-dependent effects.

5. Magnetic field effects

In this section we describe the effect of the external magnetic field H on the spectra for different values of the exchange field x. We will see that since the effect of the magnetic field depends on the spin, the evolution of the tunnelling spectra with x is asymmetric. The tunnelling conductance is given by

$$\sigma_q(E) = \sigma_{q_\uparrow}(E - \mu_B H) + \sigma_{q_\downarrow}(E + \mu_B H). \tag{24}$$

In figures 7(a), 7(b), 7(c) the tunnelling conductance $\sigma_q(E)$ is plotted for fixed magnetic field $\mu_B H/\Delta_0 = 1$ and barrier strength $z_0 = 2.5$, for different values of the exchange interaction x. The pairing symmetry of the superconductor is $B_{1g} \times E_u$, $B_{2g} \times E_u$, nodal p wave, respectively. The same information is plotted in figures 8(a), 8(b), for the nodeless pairing states: isotropic

p wave and p wave proposed by Miyake and Narikiyo [21], respectively. The orientation of the superconductor is chosen as $\beta = 0$. In the absence of the exchange interaction ($x = 0$) the magnetic field splits the tunnelling spectrum symmetrically. The amplitude of the splitting depends linearly on the magnetic field H. The main effect of the polarization is the imbalance in the peak heights for E positive and negative. The ratio of the peaks for positive and negative energy is proportional to the exchange field of the material. For $E < 0$ the pattern is suppressed linearly with the increase of x, while for $E > 0$ the tunnelling conductance spectrum initially increases with x and then decreases. Also the conclusions of the previous section for the nodal and nodeless forms of the tunnelling spectra are still valid in the presence of a magnetic field.

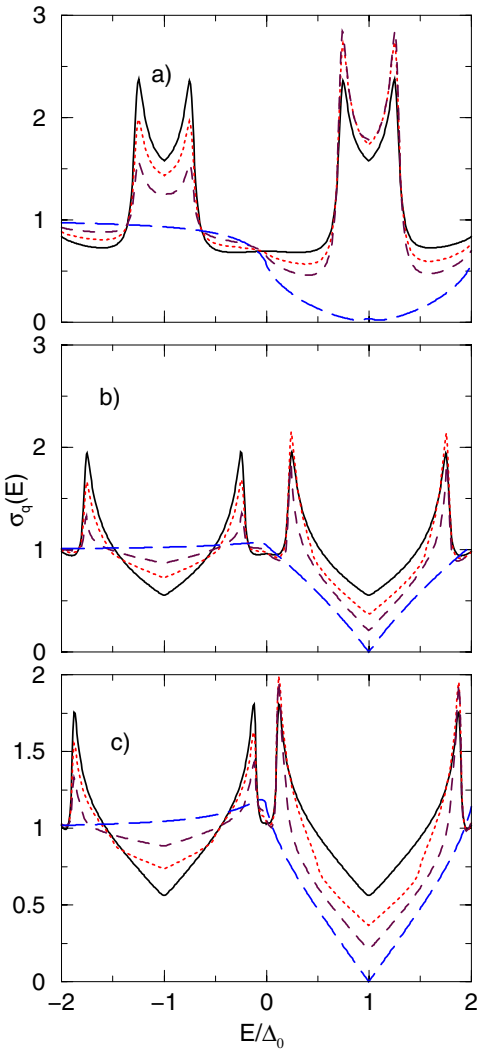

Figure 7. Normalized tunnelling conductance $\sigma_q(E)$ as a function of E/Δ_0 for $x = 0$ (solid line), $x = 0.2$ (dotted line), $x = 0.4$ (dashed line), and $x = 0.999$ (long-dashed line), for $z_0 = 2.5$, $\beta = 0.0$, $\mu_B H/\Delta_0 = 1$, for different nodal pairing states: (a) $B_{1g} \times E_u$, (b) $B_{2g} \times E_u$, (c) nodal p wave.

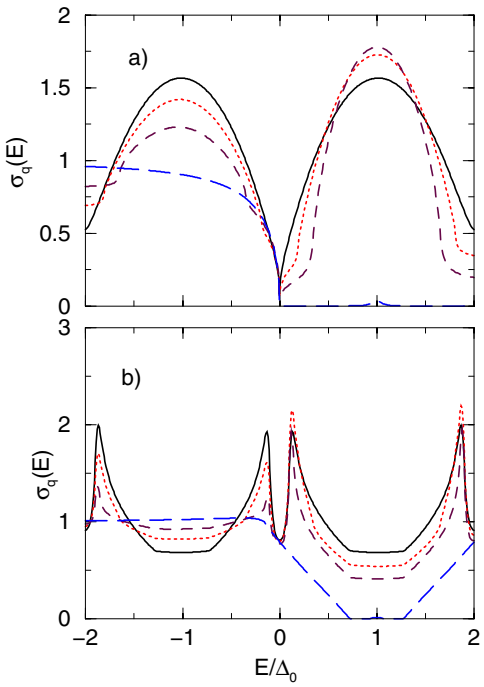

Figure 8. Normalized tunnelling conductance $\sigma_q(E)$ as a function of E/Δ_0 for $x = 0$ (solid line), $x = 0.2$ (dotted line), $x = 0.4$ (dashed line), and $x = 0.999$ (long-dashed line), for $z_0 = 2.5$, $\beta = 0.0$, $\mu_B H/\Delta_0 = 1$, for different nodeless pairing states: (a) isotropic p wave, (b) nodeless p wave proposed by MN.

6. Conclusions

We have calculated the tunnelling conductance in ferromagnet/insulator/triplet-superconductor junctions, using the BTK formalism. We assumed pairing potentials with nodes such as the nodal p-wave state and two 2D f-wave states with line nodes, breaking the time-reversal symmetry. Also we examined two nodeless pairing states, the p wave proposed by Miyake and Narikiyo [21] and the isotropic p wave. The linear variation of the conductance with E is an indication of line nodes and is not influenced much when the exchange interaction increases. On the other hand, the large residual density of states within the gap is reduced with the increase of x, and the peaks due to the formation of bound states are removed due to the suppression of the Andreev reflection. The evolution of the spectra with x depends on the position of the nodes and the orientation angle β and is different for the three pairing states with line nodes. In the case of nodeless pairing states, the tunnelling conductance develops a subgap or a full gap within which $\sigma_q(E)$ has a constant value. The exchange interaction suppresses the conductance within the gap, and can be considered as a measure of the polarization of the material. The magnetic field splits the tunnelling spectra linearly, and in the half-metallic ferromagnetic limit $x = 1$, eliminates the negative branch of the spectrum. These features can be used to distinguish between the candidate pairing symmetry states of Sr_2RuO_4.

References

[1] Maeno Y, Hashimoto H, Yoshida K, Nishizaki S, Fujita T, Bednorz J G and Lichtenberg F 1994 *Nature* **372** 532
[2] Luke G M, Fukamoto Y, Kojima K M, Larkin M L, Merrin J, Nachumi B, Uemura Y J, Maeno Y, Mao Z Q, Mori Y, Nakamura H and Sigrist M 1998 *Nature* **394** 558
[3] Ishida K, Mukuda H, Kitaoka Y, Asayama K, Mao Z Q, Mori Y and Maeno Y 1998 *Nature* **396** 658
[4] Mazin I I and Singh D J 1997 *Phys. Rev. Lett.* **79** 733
[5] Mackenzie A P, Ikeda S, Maeno Y, Fujita T, Julian S R and Lonzarich G G 1998 *J. Phys. Soc. Japan* **67** 385
[6] Ishida K, Kitaoka Y, Asayama K, Ikeda S, Nishizaki S, Maeno Y, Yoshida K and Fujita T 1997 *Phys. Rev.* B **56** 505
[7] Nishizaki S, Maeno Y and Mao Z 2000 *J. Phys. Soc. Japan* **69** 572
[8] Blonder G E, Tinkham M and Klapwijk T M 1982 *Phys. Rev.* B **25** 4515
[9] Andreev A F 1964 *Sov. Phys.–JETP* **19** 1228
[10] Tanaka Y and Kashiwaya S 1995 *Phys. Rev. Lett.* **74** 3451
[11] Covington M, Aprili M, Paraoanu E, Green L H, Xu F, Zhu J and Mirkin C A 1997 *Phys. Rev. Lett.* **79** 277
[12] Stefanakis N 2001 *J. Phys.: Condens. Matter* **13** 1265
[13] Dimoulas A 2000 *Phys. Rev.* B **61** 9729
[14] de Jong M J M and Beenakker C W J 1995 *Phys. Rev. Lett.* **74** 1657
[15] Kashiwaya S, Tanaka Y, Yoshida N and Beasley M R 1999 *Phys. Rev.* B **60** 3572
[16] Zhu J-X, Friedman B and Ting C S 1999 *Phys. Rev.* B **59** 9558
[17] Yoshida N, Tanaka Y, Inoue J and Kashiwaya S 1999 *J. Phys. Soc. Japan* **68** 1071
[18] Maki K and Haas S 2000 *Preprint* cond-mat/0008095
[19] Hasegawa Y, Machida K and Ozaki M 2000 *J. Phys. Soc. Japan* **69** 336
[20] Dahm T, Won H and Maki K 2000 *Preprint* cond-mat/0006301
[21] Miyake K and Narikiyo O 1999 *Phys. Rev. Lett.* **83** 1423
[22] Graf M J and Balatsky A V 2000 *Preprint* cond-mat/0005546
[23] Sigrist M and Ueda K 1991 *Rev. Mod. Phys.* **63** 239
[24] Honerkamp C and Sigrist M 1998 *J. Low Temp. Phys.* **111** 898
[25] Bruder Cr 1990 *Phys. Rev.* B **41** 4017
[26] Stefanakis N 2001 *Preprint*
[27] Stefanakis N 2001 *Preprint*